# New Linear and Star-Shaped Thermogelling Poly([ R ]-3-hydroxybutyrate) Copolymers

Ghislaine Barouti, Sing Shy Liow, Qingqing Dou, Hongye Ye, Clément Orione, Sophie M. Guillaume, Xian Jun Loh

**New linear and star-shaped thermogelling poly([*R*]-3-hydroxybutyrate) copolymers**

Ghislaine Barouti,[1,2] Sing Shy Liow,[2] Qingqing Dou,[2] Hongye Ye[2], Clément Orione,[3] Sophie M. Guillaume,[1,*] Xian Jun Loh[2,4,5*]

1. Institut des Sciences Chimiques de Rennes, UMR 6226 CNRS - Université de Rennes 1, Campus de Beaulieu, 263 Avenue du Général Leclerc, F-35042 Rennes Cedex, France
2. Institute of Materials Research and Engineering (IMRE), 3 Research Link, Singapore 117602 Singapore
3. Centre Régional de Mesures Physiques de l'Ouest, Université de Rennes 1, Campus de Beaulieu, F-35042 Rennes Cedex, France
4. Department of Materials Science and Engineering, National University of Singapore, 9 Engineering Drive 1, Singapore 117576, Singapore
5. Singapore Eye Research Institute, 11 Third Hospital Avenue, Singapore 168751, Singapore

Corresponding authors: lohxj@imre.a-star.edu.sg; sophie.guillaume@univ-rennes1.fr

**Abstract**

The synthesis of multi-arm PHB-based triblock copolymers (poly([*R*]-3-hydroxybutyrate)-*b*-poly(*N*-isopropylacrylamide)-*b*-[[poly(methyl ether methacrylate)-*g*-poly(ethylene glycol)]-*co*-[poly(methacrylate)-*g*-poly(propylene glycol)]], PHB-*b*-PNIPAAM-*b*-(PPEGMEMA-*co*-PPPGMA), and their subsequent self-assembly into thermoresponsive hydrogels are described. ATRP of *N*-isopropylacrylamide (NIPAAM) followed by poly(ethylene glycol) methyl ether methacrylate (PEGMEMA) and poly(propylene glycol) methacrylate (PPGMA), was achieved from bromoesterified multi-arm PHBs macroinitiators. The composition of the resulting copolymers was investigated by $^{1}$H, $^{13}$C J-MOD NMR, SEC, TGA, and DSC analyses. Copolymers featuring different architectures and distinct hydrophilic/hydrophobic contents were found to self-assemble into thermoresponsive gels in aqueous solution. Rheological studies indicated that the linear 1-arm based copolymer tend to form a micellar solution, while 2- and 4-arm copolymers afforded gels with enhanced mechanical properties and solid-like behavior. These investigations are the first to correlate the gelation properties to the arm-number of a PHB-based copolymer. All copolymers revealed a double thermoresponsive behavior due to the NIPAAM and PPGMA blocks, thus allowing first the copolymer self-assembly at room temperature, and then the delivery of a drug at body temperature (37 °C). The non-significant toxic response of the gels, as assessed by cell viability of CCD-112CoN human fibroblast cell lines with different concentrations of the triblock copolymer ranging from 0.03 to 1 mg.mL$^{-1}$, suggest that these PHB-based thermoresponsive gels are promising candidate biomaterials for drug delivery applications.

**Keywords:** Poly([*R*]-3-hydroxybutyrate) (PHB), multi-arm polymer, water-soluble polymer, thermo-responsive polymer, hydrogel, drug delivery, polyester

**Graphical abstract**

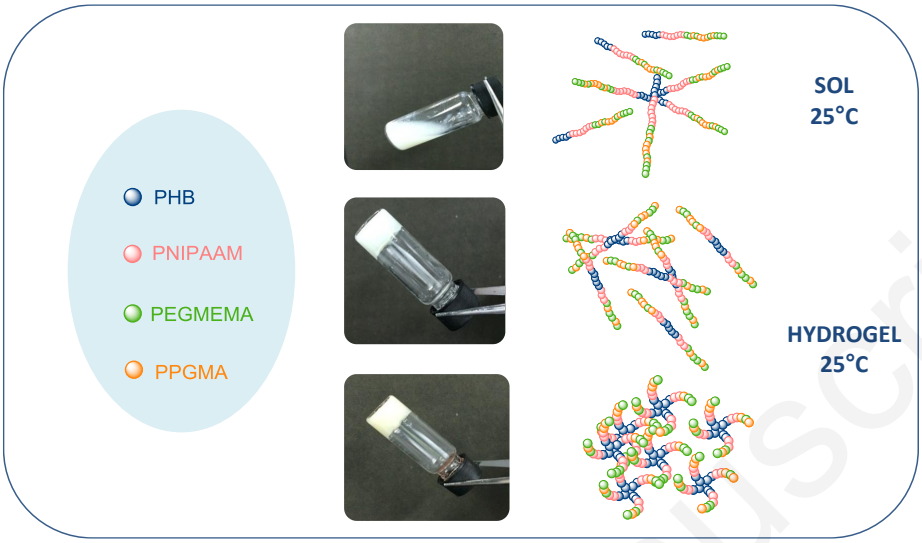

**Introduction**

Supramolecular hydrogels belong to a novel class of three-dimensional hydrophilic cross-linked polymers possessing display unique physicochemical properties such as, water swelling capabilities, therapeutic encapsulation, biodegradability and biocompatibility. They also display interesting properties such as optoelectronic properties, enzyme responsiveness, self-healing ability and shape memory properties.[1] Some hydrogels are also able to undergo reversible phase transition in response to various environmental stimuli due to the noncovalent cross-linkages and can be used as promising biomaterial scaffolds for diagnosis and therapeutic delivery.[1d, 2] Thermoresponsive hydrogels are an important class of soft supramolecular materials that are suitable for a wide range of biomedical applications, such as injectable *in-situ* gelling drug release depots,[3] tissue engineering scaffolds,[4] cell sheet engineering,[5] and anti-adhesion materials.[6] They consist of chemically or physically crosslinked three dimensional polymeric networks, that can hold a large amount of water without breakdown. These high water content hydrogels also allow these hydrogels to be used for 3D cell culture. Thermoresponsive hydrogels,[2f] also referred to as thermogels, undergo a sol-gel transition as the temperature changes.[2e] Notably, thermogels have potential applications in injectable systems and nanomedicine due to their ability to self-assemble into micelles in an aqueous medium.[7] At body temperature (37 ˚C), hydrophobic segments such as poly([*R*]-3-hydroxybutyrate) (PHB),[8] poly(propylene glycol) (PPG),[9] poly(ε-caprolactone-*co*-lactide) (PCLA),[10] and poly(*D,L*-lactide-*co*-glycolide) (PLGA),[11] are used to form the core of the micelles, while hydrophilic segments such as the common poly(ethylene glycol) (PEG) interact with water molecules at the corona. The driving force for a sol-gel transition are the hydrophobic interactions which are favored at higher temperatures. The association of hydrophobic cores forces ordered packing of micelles into a macroscopic gel.[12]

Among such hydrophobic cores, natural PHB is a linear, biodegradable and biocompatible isotactic polyester featuring *D*(−)-3-hydroxybutyric acid as repeating unit. PHB thus belongs to the class of natural renewable polymers derived from the biomass, similar to lignin, cellulose, starch or plant oils which are originated from green and sustainable resources.[13] PHB is also the most common member of the polyhydroxyalkanoate (PHA) family, which are aliphatic polyesters featuring a three-carbon backbone structure with a substituent (R) on the β-position (Figure 1; R = Me for PHB).[14]

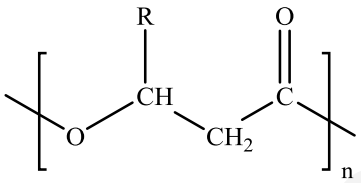


**Figure 1.** Chemical structure of PHAs

As a hydrophobic and semi-crystalline polymer, PHB is hard to dissolve in common organic solvents, it is also brittle as compared to other biodegradable polyesters such as poly(ε-caprolactone) (PCL).[15] These drawbacks keep PHB away from a wide range of applications, especially in the field of water-soluble polymers and hydrogels. To date, studies reported on PHB-based hydrogels remain limited. The polyurethane approach involving the reaction of a PHB diol with a diisocyanate, provides a convenient synthetic pathway to produce biodegradable PHB-based thermogels with 98 wt.% of water from a polymer concentration as low as 2 wt.%.[8a] Also, atom transfer radical polymerization (ATRP) process was used to prepare thermo-responsive PHB copolymers based on poly(*N*-isopropyacrylamide), PNIPAAM-*b*-PHB-*b*-PNIPAAM,[8c] and an esterification reaction was used to prepare PHB-*b*-PEG-*b*-PHB[16] and PEG-*b*-PHB-*b*-PEG[8b] triblock copolymers, affording thermo-responsive micelles. However these copolymers could not form a hydrogel at physiological temperature, probably due to the unbalanced hydrophobicity-hydrophilicity.

Both the PHB-*b*-PEG-*b*-PHB[16] and PEG-*b*-PHB-*b*-PEG[8b] triblock copolymers were formulated with an α-cyclodextrin solution to afford hydrogels based on supramolecular interactions. These latter hydrogels resulted from the aggregation of α-cyclodextrin and PEG segments, and were found suitable for controlled drug release applications. A recent study reported symmetric star shape PHB (~100 kDa) prepared by ring-opening polymerization. The relationship between solution and melt viscosity of PHB with linear and star (3-arm and 6-arm) were therein demonstrated.[17]

The present study reports the synthesis of first PHB oligomers with 1, 2, and 4 hydroxyl end-capping groups from commercially available natural PHB, using different transesterification agents such as hexanol, ethylene glycol and erythritol (PHB1-OH, PHB2-OH and PHB4-OH, respectively), and their ensuing bromoesterification (Scheme 1). Subsequently, these latter PHBs-Br served as macroinitiators for the ATRP of first (*N*-isopropylacrylamide) (NIPAAM) to provide diblock PHB-*b*-PNIPAAM copolymers, and consequently of poly(ethylene glycol) methyl ether methacrylate (PEGMEMA) and poly(propylene glycol) methacrylate (PPGMA), to ultimately afford a series of PHB-based thermo-responsive triblock copolymers, PHB-*b*-PNIPAAM-*b*-(PPEGMEMA-*co*-PPPGMA) (Scheme 2). The copolymers consisted of a central organic core and of several arms of copolymer chains composed of blocks of PHB, PNIPAAM and a last block of randomly distributed PPEGMEMA and PPPGMA, the latter acrylate segments bearing PEG and PPG grafts, respectively. Linear and star-shaped copolymers derived from PHB1, and PHB2 or PHB4, respectively, provided thermo-responsive hydrogels as evidenced by rheological investigations in relation to the number of arms and the hydrophilic/hydrophobic content. Cytotoxicity assay and doxorubicin release monitoring showed these novel triblock copolymers to be promising drug-delivery systems.

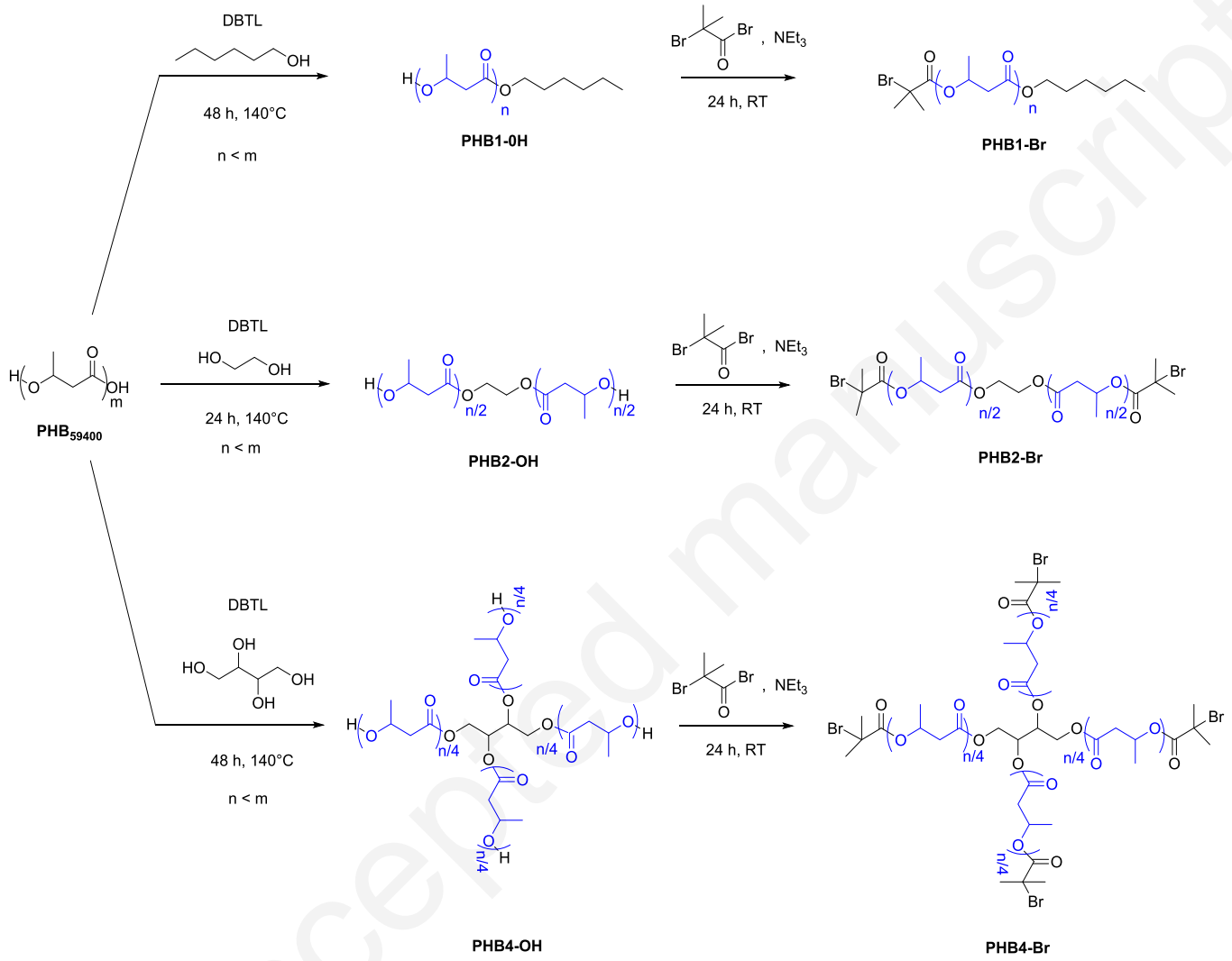


**Scheme 1.** Synthesis of multi-arm hydroxy telechelic PHBs from the transesterification of high molar mass PHB followed by bromoesterification.

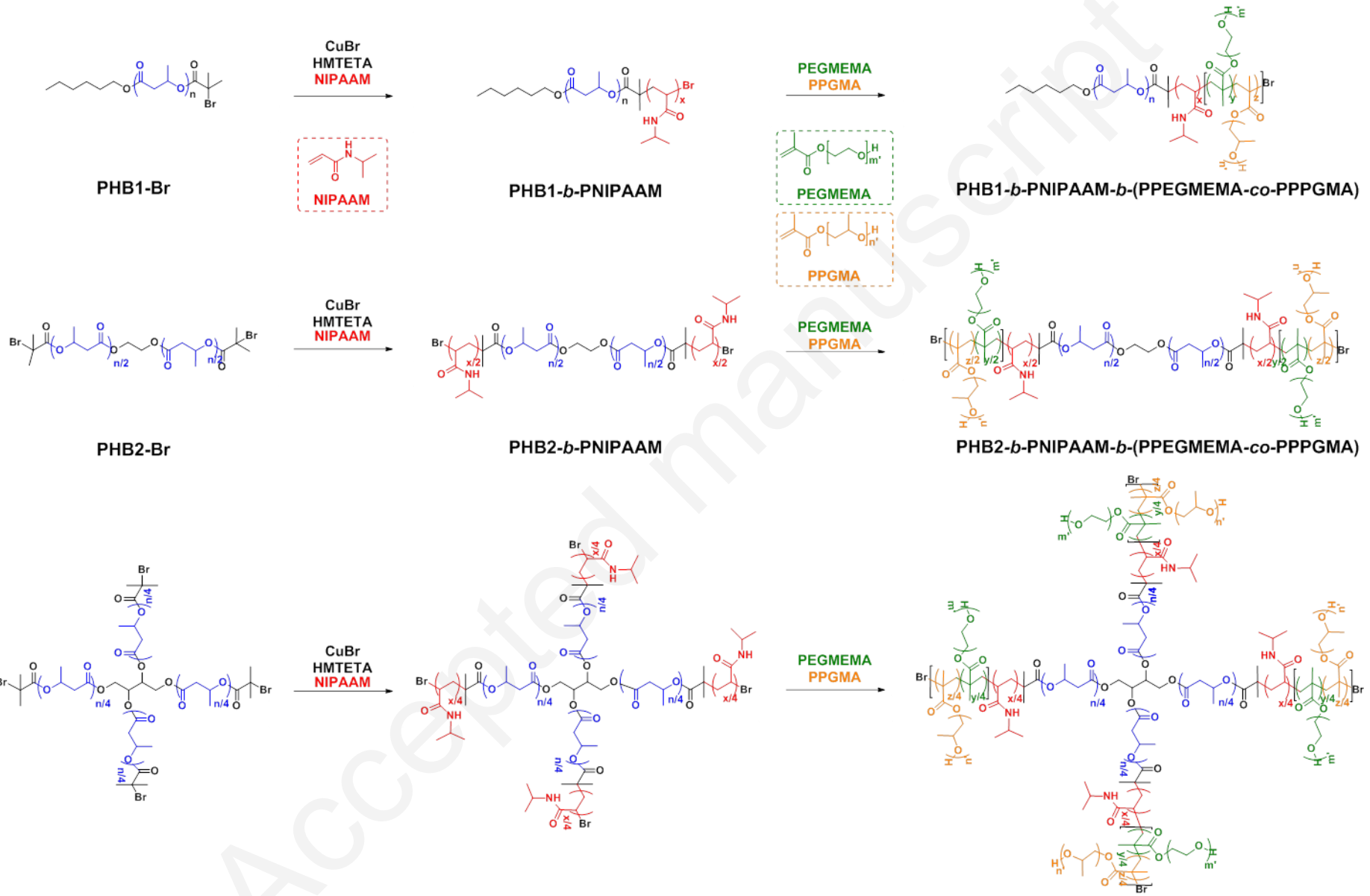

**Scheme 2.** Synthesis of PHB-*b*-PNIPAAM-*b*-(PPEGMEMA-*co*-PPPGMA) by sequential ATRP of NIPAAM followed by a one-pot ATRP of PEGMEMA and PPGMA from multi-arm hydroxy telechelic PHB macroinitiators.

## Results and discussion

**Synthesis and characterization of multi-arm PHBs as ATRP macroinitiators.** Multi-arm hydroxyl end-capped PHBs were synthesized from the transesterification of a high molar mass natural PHB with different alcohols, namely hexanol, ethylene glycol and erythritol, in the presence of dibutyl tin dilaurate (DBTL) catalyst, as inspired by a previously reported procedure (Scheme 1)[18]. The recovered purified hydroxy telechelic PHBs, PHB1-OH, PHB2-OH and PHB4-OH, respectively, were then characterized by $^1$H NMR analyses (refer to the Experimental Section, Figures S1–S3). A series of three PHBs-OH having 1, 2 or 4 arms, i.e. 1, 2 or 4 terminal hydroxyl groups, and with a molar mass of $M_{n,NMR}$ = 1600, 2300 and 1700 g.mol$^{-1}$, respectively, were isolated in fair yields (Table S1). These hydroxy end-functionalized pre-oligomers were next chemically modified into their analogous bromoester end-capped PHBs (Scheme 1), to subsequently serve as ATRP macroinitiators in the successive polymerization of the acrylamide and methacrylates (Scheme 2). The esterification of PHBs-OH using 2-α-bromoisobutyryl bromide afforded the corresponding PHBs-Br without alteration of the polyester backbone, as monitored by $^1$H NMR analyses (Table S1, Figures S4–S6). It needs to be further noted that the hydroxylated PHBs and the subsequent brominated PHBs have a polydispersity ranging from 1.3 to 1.5, indicating that the subsequent copolymers actually cover a range of molecular weights and may be made from polymers of different chain length.

**Synthesis and characterization of PHB-*b*-PNIPAAM-*b*-(PPEGMEMA-*co*-PPPGMA) copolymers.** The synthesis of poly(3-hydroxybutyrate)-*b*-poly(*N*-isopropylacrylamide)-*b*-[[poly(methyl ether methacrylate)-*g*-poly(ethylene glycol)]-*co*-[poly(methacrylate)-*g*-

poly(propylene glycol)]] (PHB-*b*-PNIPAAM-*b*-(PPEGMEMA-*co*-PPPGMA) was easily synthesized from PHBs-Br following a stepwise approach (Scheme 2). The PHB-*b*-PNIPAAM diblock copolymers were first synthetized from the PHBs-Br macroinitiators by ATRP of NIPAAM catalyzed by CuBr. NMR molar mass values ($M_{n,NMR}$) of PHB-*b*-PNIPAAM copolymers was in good agreement with the theoretical data ($M_{n,th}$) as determined from the monomer consumption (Table 1). For instance, NMR monitoring of the polymerization of NIPAAM from PHB1-Br into the corresponding PHB1-*b*-PNIPAAM, showed the linear increase of the molar mass of the PNIPAAM segment as determined from $^1$H NMR analysis of the isolated diblock copolymer, with the NIPAAM conversion, as depicted in Figure 2. Along with the fair agreeement of the molar mass as determined by $^1$H NMR spectrocopy ($M_{n,NMR}$, Table 1), with the theroetical molar mass value as calculated from the NIPAAM conversion ($M_{n,theo}$, Table 1), this behavior contributed to highlight a controlled polymerization.

**Table 1.** ATRP of NIPAAM, PEGMEMA and PPGMA from PHBs-Br macroinitiators.

| Copolymer | $[PHB–Br]_0$ : $[CuBr]_0$ : $[NIPAAM]_0$ : $[PEGMEMA]_0$ : $[PPGMA]_0$ | Number of PHB arm | PHB-Br $M_{n,NMR}$ [a] (g.mol$^{-1}$) | NIPAAM Conv. [b] (%) | PNIPAAM $M_{n,th}$ [c] (g.mol$^{-1}$) | PNIPAAM $M_{n,NMR}$ [d] (g.mol$^{-1}$) | PPEGMEMA $M_{n,th}$ [e] | PPPGMA $M_{n,th}$ [e] | PPEGMEMA: PPPGMA molar mass ratio[f] (%) | PHB:PNIPAAM: PPEGMEMA: PPPGMA molar mass ratio[g] (%) | PHB: PNIPAAM: PPEGMEMA: PPPGMA $M_{n,th}$[h] | PHB-*b*-PNIPAAM-*b*-(PPEGMEMA-*co*-PPPGMA) $M_{n,SEC}$ [i] | $Đ_M$ [j] |
|---|---|---|---|---|---|---|---|---|---|---|---|---|---|
| P1 | 1:1:100:9:14 | 1 | 1400 | 55 | 6200 | 6000 | 9900 | 5200 | 2:1 | 6:27:44:23 | 22 500 | 26 300 | 1.78 |
| P2 | 1:1:70:9:14 | 2 | 2500 | 89 | 7050 | 7000 | 9900 | 5200 | 2:1 | 10:28:41:21 | 24 600 | 18 850 | 1.71 |
| P3 | 1:1:70:7:20 | 2 | 2500 | 72 | 5700 | 5700 | 7700 | 7500 | 1:1 | 11:24:33:32 | 23 400 | 20 000 | 1.48 |
| P4 | 1:1:70:11:8 | 2 | 2500 | 58 | 4900 | 4600 | 12100 | 3000 | 4:1 | 11:20:55:14 | 22 200 | 17 300 | 1.71 |
| P5 | 1:1:55:9:14 | 4 | 1700 | 79 | 4900 | 5000 | 9900 | 5200 | 2:1 | 8:23:45:24 | 21 800 | 17 700 | 1.88 |

[a] Experimental molar mass value of PHB-Br determined by $^1$H NMR analysis in $CDCl_3$ of the isolated polymer (*not including* either the $–C(O)C(CH_3)_2Br$ or the alcohol moiety $–(CH_2)_5CH_3$, $–O(CH_2)_2O–$ or $–OCH_2(CH(O))_2CH_2O$ for PHB1, PHB2 and PHB4, respectively; refer to the Experimental Section, Table S1). [b] NIPAAM conversion determined by $^1$H NMR analysis of the crude reaction mixture (refer to the Experimental Section). [c] Theoretical molar mass value of the PNIPAAM segment of the PHB-*b*-PNIPAAM diblock copolymer calculated from the relation: $[[NIPAAM]_0/[PHB–Br]_0 \times Conv_{NIPAAM} \times M_{NIPAAM}]$ with $M_{NIPAAM}$ = 113 g.mol$^{-1}$. [d] Experimental molar mass value of PNIPAAM segment of the PHB-*b*-PNIPAAM diblock copolymer determined by $^1$H NMR analysis in $CDCl_3$ of the isolated polymer from the relative intensities of the signals of the the methylene ($–CH_2CH(CONH(CH_3)_2)$, δ 2.51 ppm) to the PHB main-chain methine hydrogens ($–OCH(CH_3)CH_2$, δ 5.26 ppm)(refer to experimental section).[e] PPEGMEMA and PPPGMA theoretical molar mass values calculated from the relation: $[[PEGMEMA]_0/[PHB\text{-}b\text{-}PNIPAAM\text{-}Br]_0 \times Conv_{PEGMEMA} \times M_{PEGMEMA}]$ with $M_{PEGMEMA}$ = 1100 g.mol$^{-1}$ and $[[PPGMA]_0/[PHB\text{-}b\text{-}PNIPAAM\text{-}Br]_0 \times Conv_{PPGMA} \times M_{PPGMA}]$, respectively, with $M_{PPGMA}$ = 375 g.mol$^{-1}$, assuming the quantitative conversion of PEGMEMA and PPGMA (refer to the Experimental Section). [f] Molar mass ratio of the PPEGMEMA and PPPGMA blocks of the copolymer as determined from the initial monomer feed ratio. [g] Molar mass ratio of the PHB, PNIPAAM, PPEGMEMA and PPPGMA blocks of the copolymer as determined from $M_{n,NMR}$ for PHB and PNIPAAM and from $M_{n,th}$ for PPEGMEMA and PPPGMA. [i] Theoretical molar mass values of the triblock copolymer determined from the relation: $M_{n,NMR,PHB} + M_{n,NMR,PNIPAAM} + M_{n,th,PPEGMEMA} + M_{n,th,PPPGMA}$. [i] Experimental molar mass values determined by SEC analysis in THF at 30 °C *vs.* polystyrene standards (uncorrected value; refer to the Experimental Section). [j] Dispersity value determined by SEC analysis in THF at 30 °C.

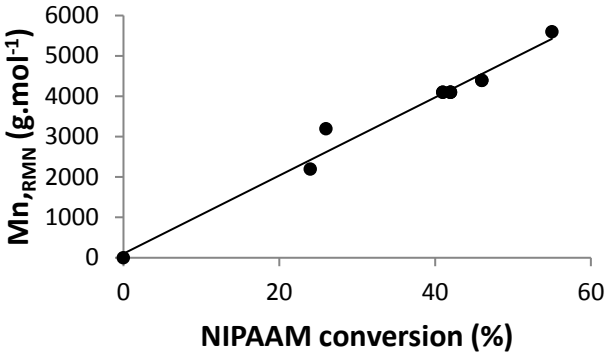


**Figure 2.** Variation of $M_{n,NMR}$ (g.mol$^{-1}$) values of the PNIPAAM segment in the PHB-*b*-PNIPAAM diblock copolymer, synthesized from PHB1-Br macroinitiator, as a function of NIPAAM conversion (Table 1, entry 1).

Incorporation of both PEGMEMA and PPGMA was clearly evidenced by $^{1}$H NMR analysis, as illustrated in Figure 3 (Figures S7, S8). For the 2-arm PHB-based copolymer, the PEGMEMA/PPGMA feeding ratio was varied from 1:1 to 4:1 in order to evaluate the physico-chemical properties of the subsequent gels derived from the triblock copolymers upon varying the hydrophilic/hydrophobic content. A set of five distinct PHB-*b*-PNIPAAM-*b*-(PPEGMEMA-*co*-PPPGMA) with 1, 2 or 4 arms and different PEGMEMA/PPGMA ratios was thus prepared with similar molar mass value ($M_{n,th}$ = 21 800–24 600 g.mol$^{-1}$), and isolated in a grams scale (typically ca. 3 g). The chemical structure of the resulting PHB-*b*-PNIPAAM-*b*-(PPEGMEMA-*co*-PPPGMA) triblock copolymers was assessed by $^{1}$H NMR (Figure 3, S7, S8) after purification of the copolymers by dialysis. The corresponding $^{13}$C[$^{1}$H] J-MOD NMR spectra similarly evidenced the characteristic signals of PHB, PNIPAAM, PPEGMEMA and PPPGMA segments along with their respective awaited phase (Figure 4). The isolated triblock copolymers exhibited a monomodal SEC chromatogram with molar mass values up to $M_{n,SEC}$ = 26 300 g.mol$^{-1}$ and relatively moderate dispersity (1.48 < $Đ_M$ < 1.88; Table 1).

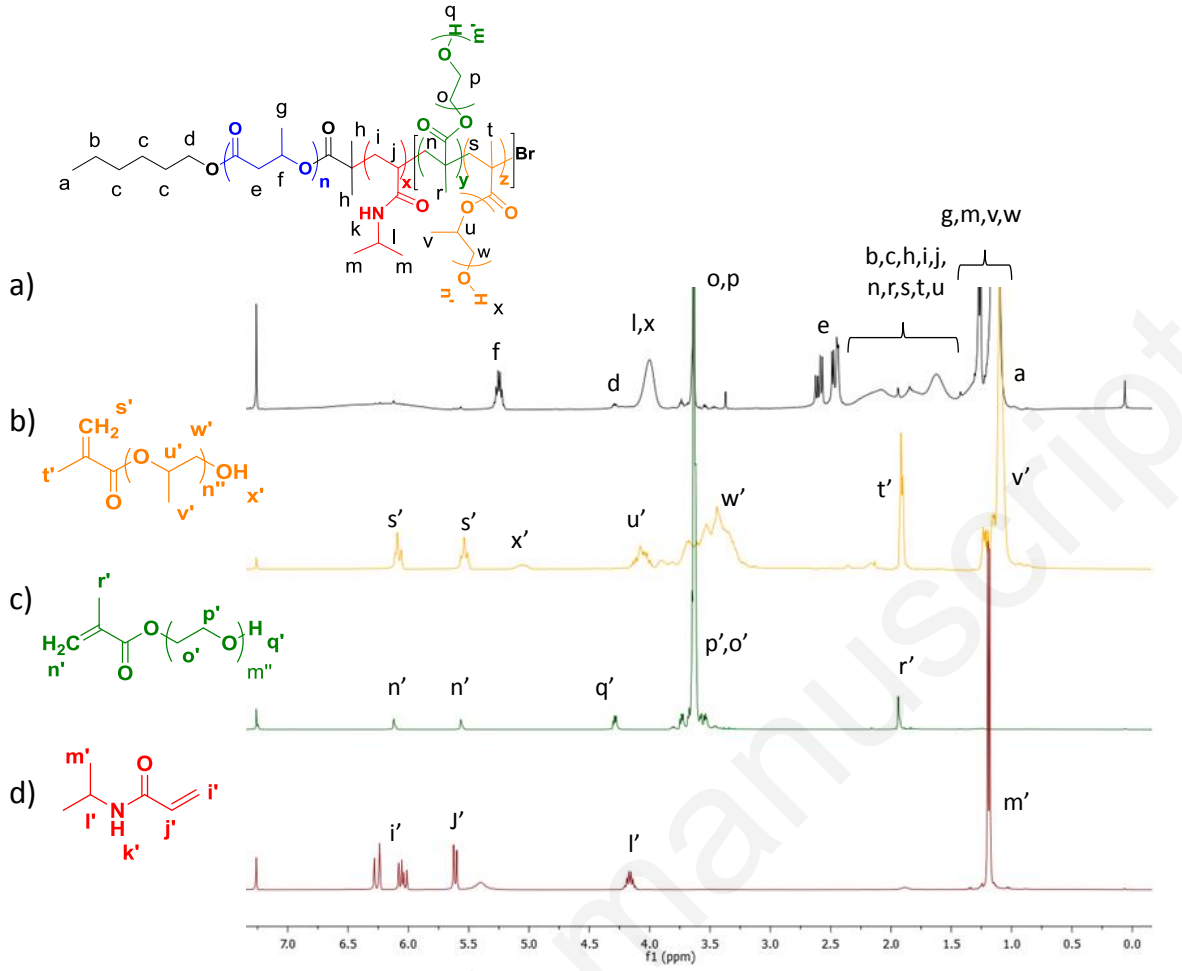


**Figure 3.** $^{1}$H NMR (400 MHz, $CDCl_3$, 23 °C) spectra of: a) $PHB1_{1400}$-*b*-$PNIPAAM_{6000}$-*b*-($PPEGMEMA_{9900}$-*co*-$PPPGMA_{5200}$) (Table 1, entry 1) synthesized by the ATRP of NIPAAM from $PHB1_{1400}$–Br (Table S1, entry 1), followed by the random ATRP of PEGMEMA and PPGMA; b) PPGMA ($M_n$ = 375 g.mol$^{-1}$), c) PEGMEMA ($M_n$ =1100 g.mol$^{-1}$), and d) NIPAAM.

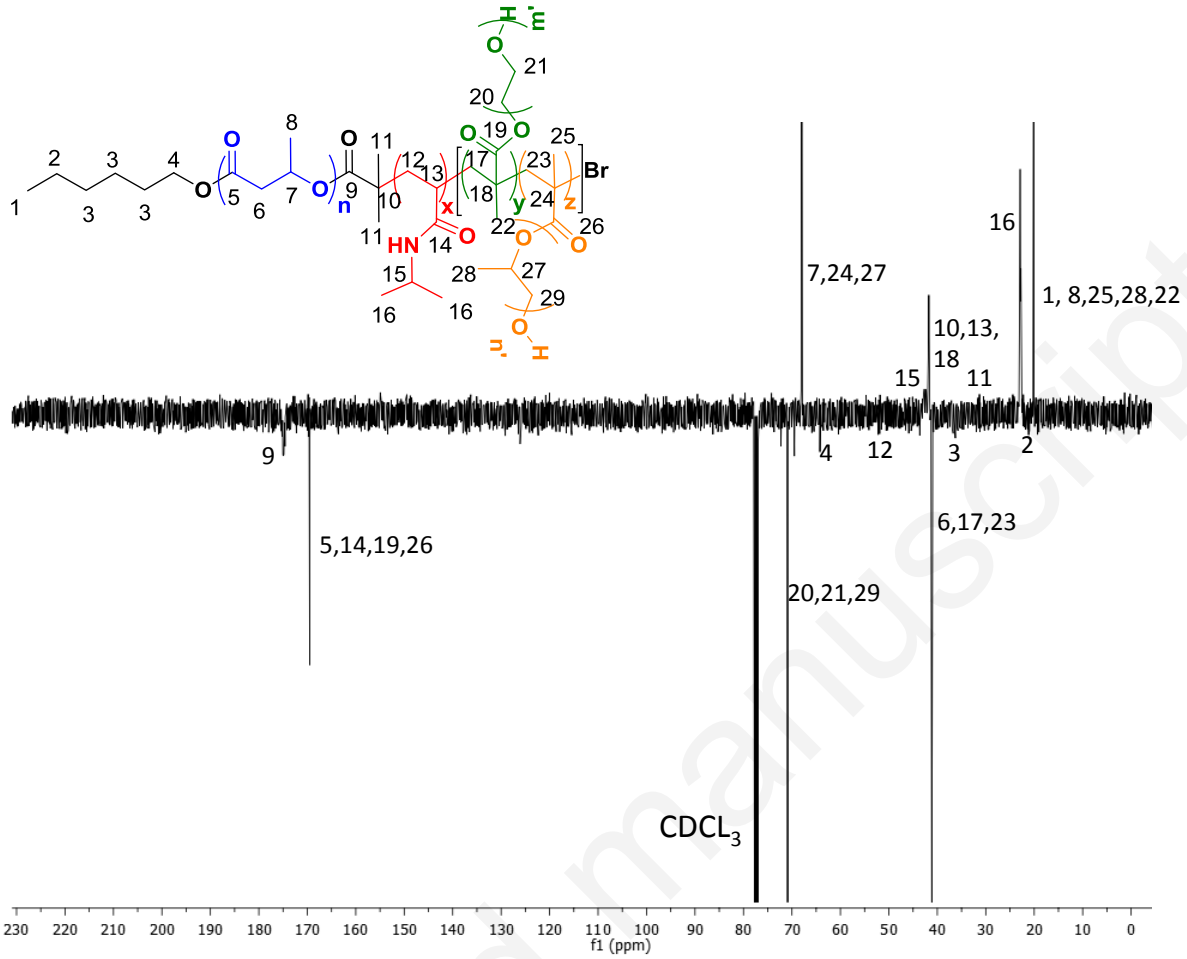


**Figure 4.** $^{13}C[^{1}H]$ J-MOD NMR (100 MHz, $CDCl_3$, 23 °C) spectrum of $PHB1_{1400}$-*b*-$PNIPAAM_{6000}$-*b*-($PPEGMEMA_{9900}$-*co*-$PPPGMA_{5200}$) (Table 1, entry 1) synthesized by the ATRP of NIPAAM from $PHB1_{1400}$–Br (Table S1, entry 1), followed by the ATRP of PEGMEMA and PPGMA.

The thermal characteristics of the triblock copolymers featuring a different number of arms and of PPEGMEMA/PPPGMA contents, were estimated by TGA analyses, as illustrated in Figure 5. The thermal degradation profiles of all the copolymers featuring a similar molar mass value ($M_{n,th}$ = ca. 22 900 g.mol$^{-1}$) were similar regardless of the number of arms. The analyses revealed their thermal stability up to *ca.* 250 °C, which is suitable for auto-claving (usually at 121 °C). The observed two-step mass loss profile was attributed to the stepwise

quantitative thermal degradation of the PHB-*b*-PNIPAAM-*b*-(PPEGMEMA-*co*-PPPGMA), with the first step occurring between *ca.* 250 °C and 325 °C, followed by the second step from *ca.* 325 °C to 445 °C. These two stages of mass reduction were assigned to the degradation of first the PHB segment and part of the PPPGMA block ($T_d^{25}$ = ca. 276 °C; temperature at which 25 % of the triblock copolymer mass loss has occurred), prior to that of the PNIPAAM, PPEGMEMA and remaining PPPGMA segments ($T_d^{75}$ = ca. 404 °C; temperature at which 75 % of copolymer mass loss has occurred), respectively, as illustrated with the profile of PHB2-*b*-PNIPAAM-*b*-(PPEGMEMA-*co*-PPPGMA) (P3; Figure 5). Indeed, the onset degradation temperature of bacterial PHB has been reported at $T_d$ = 229 °C[19], while PHB1-OH, PNIPAAM, PEGMEMA and PPGMA have shown degradation temperature, $T_d^{25}$ at ca. 289 °C, 400 °C,[20] 398 °C and 241 °C , respectively (Figure 5-traces,a,c,d).

**Table 2.** Thermal characteristics of PHB-*b*-PNIMAAM-*b*-(PPEGMEMA-*co*-PPPGMA) copolymers

| Reference | PHB:PNIPAAM: PPEGMEMA:PPPGMA Molar ratio[a] | $T_m$[b] (°C) | $T_m$[b] (°C) | $T_{d1}$[c] (°C) | Weight loss[d] (%) | $T_{d2}$[c] (°C) | Weight loss[d] (%) |
|---|---|---|---|---|---|---|---|
| P1 | 5:27:45:23 | 35 | 135 | 300 | 17 | 395 | 83 |
| P2 | 10:28:41:21 | 38 | 142 | 280 | 20 | 407 | 80 |
| P3 | 11:24:33:32 | 36 | 135 | 276 | 25 | 407 | 75 |
| P4 | 11:20:55:14 | 36 | 142 | 276 | 23 | 404 | 77 |
| P5 | 8:23:45:24 | 36 | 150 | 276 | 23 | 409 | 77 |

[a] Molar mass ratio of the PHB, PNIPAAM, PPEGMEMA and PPPGMA blocks of the copolymer as determined from $M_{n,NMR}$ for PHB and PNIPAAM and from $M_{n,th}$ for PPEGMEMA and PPPGMA. [b] Melting transition temperatures measured by DSC (2nd heating cycle). [c] Decomposition temperature measured by TGA, derivative peak value was reported. [d] Weight% loss determined by TGA. [e] Not determined.

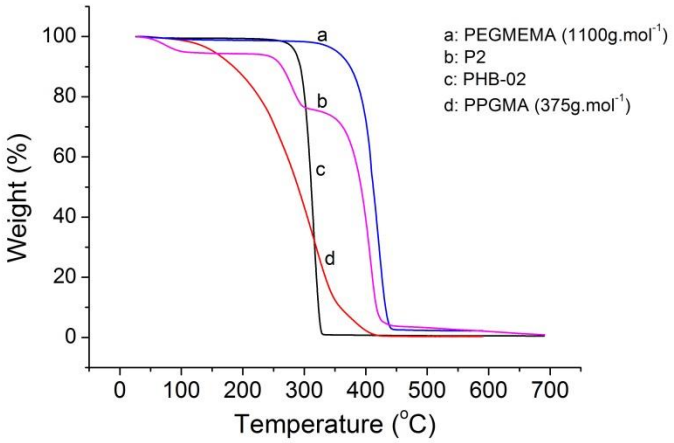


**Figure 5.** Thermal degradation profiles of a) PEGMEMA, b) P2: $PHB2_{2500}$-*b*-$PNIPAAM_{7000}$-*b*-($PPEGMEMA_{9900}$-*co*-$PPPGMA_{5200}$) (note that the first degradation observed corresponds to residual solvents loss) (Table 1, entry 2), c) PHB2-OH, and d) PPGMA. The thermal degradation profiles of PHB-*b*-PNIPAAM-*b*-(PPEGMEMA-*co*-PPPGMA) copolymers featuring different block sizes and different number of arms is reported in Figure S10).

The thermal properties of triblock copolymers were also evaluated by DSC. Results corresponding to second heating cycle only showed two thermal transtions most likely arising from the PPEGMEMA, PHB and PNIPAAM blocks (Table 2). The first melting transition temperature observed at $T_m$ = +35 – +38 °C may correspond to the PPEGMEMA segment, as the $T_m$ of the PEGMEMA precusor was recorded at +38 °C (ΔH = 110 J/g). The second thermal transition from ca. +135 °C to +150 °C resulted from the overlap of the melting transition of crystalline PHB and from the glass transition of PNIPAAM. Indeed, the mono-, di- and tetra-hydroxylated PHB macroinitiators showed a $T_m$ ranging from +130 °C to +142 °C ((ΔH = 67.8–84.5 J/g, $X_c$ = 46.3–57.6% based on reference value of 146.6 J/g for completely crystallized PHB,[21] suggesting a highly crystalline structure. This crystallinity can contribute to the observed powder morphology which is also more convenient to handle during hydrogel formulation. Furthermore, the glass transition temperature of the PNIPAAM

reported at $T_g$ = +133 °C ($M_{n,\ SEC}$ = 13300 Da) overlapped with the observed melting temperature transition at ca. 141 °C.[22] In addition, the ratio of PEGMEMA:PPGMA being fixed at 2:1 (see P1, P2 and P5), the melting enthalpies of PEGMEMA were found to lessen from ΔH = 9.1 to 0.3 J/g with an increasing number of arms. This hinted a loss of crystallinity upon raising the number of arms while keeping the PEGMEMA/PPGMA ratio constant.

**Gel formation with multi-arm PHB based copolymers.** Gels were simply formed upon dissolution of the PHB-*b*-PNIPAAM-*b*-(PPEGMEMA-*co*-PPPGMA) copolymers in water at room temperature. The effect of the number of arms in the copolymer and of the concentration of the triblock copolymer were first studied. The most significant result are gathered Table 3. The minimal required concentration to form a gel was initially established by rheological measurements at 15% (copolymer: $H_2O$, *w*/*v*) (Figure S9). These investigations revealed that gels could not be formed from the 1-arm triblock copolymer (P1) at 20%; only solutions can be formed as shown by the very low storage modulus (G'= 7.5 Pa) and loss modulus (G''= 6.9 Pa) values. On the other hand, a gel could be easily obtained from the 2-arm (P2) and the 4-arm (P5) triblock copolymers. At 20% of copolymer (*w*/*v*), the G' value measured for P5 was higher (G' = 461.5 Pa) than the one reached with P2 (G'= 63.8 Pa), thus suggesting that the star-shaped structure of the copolymer significantly and favorably enhanced the mechanical properties of the resulting gel. The PHB star-shaped structure thus seemed to nicely promote chain network interpenetration. Moreover, the PEGMEMA/PPGMA initial ratio also seemed to affect the gel properties. Indeed, hydrophobic interactions being a major driving force for gel formation, the 2-arm P3 copolymer exhibiting a PEGMEMA/PPGMA ratio of 1:1 cannot be dissolved in water due to the length of the hydrophobic block, while the P2 and P4 copolymers having a ratio of 2:1 and 4:1, respectively, did form a gel at 15% and 20% (*w*/*v*) of copolymer concentration. For the 2-arm copolymers, storage and loss modulus were higher for the gel formed with P2 copolymer

(PEGMEMA:PPGMA ratio of 2:1, G' = 63.8, G" = 35.3) than for the one formed with P4 (PEGMEMA:PPGMA ratio of 4:1, G' = 55.2, G" = 31.2). Increasing the hydrophilic content of the copolymer thus lowered the ability to form a gel.

**Table 3.** Rheological characteristics of the gels formulated from multi-arm PHB triblock copolymers at 25 °C.

| Reference | Copolymer[a] | Number of arms | Copolymer concentration[b] (*w/v*%) | G' [c] (Pa) | Visual appearance |
|---|---|---|---|---|---|
| G1 | P1 | 1 | 20 | 7.6 | sol |
| G2 | P1 | 1 | 15 | 6.8 | sol |
| G3 | P2 | 2 | 20 | 63.8 | gel |
| G4 | P2 | 2 | 15 | 29.3 | gel |
| G5 | P3 | 2 | 20 | - | insoluble |
| G6 | P3 | 2 | 15 | - | insoluble |
| G7 | P4 | 2 | 20 | 55.2 | gel |
| G8 | P4 | 2 | 15 | 6.1 | sol |
| G9 | P5 | 4 | 20 | 461.5 | gel |
| G10 | P5 | 4 | 15 | 100.3 | gel |

[a] Triblock copolymer, refer to Table 1. [b] Storage modulus measured by rheology. [c] Loss modulus measured by rheology.

In order to investigate the effect of the copolymer structure on the thermoresponsive behavior of the gels, oscillation temperature sweep experiments were performed on gels G1, G3 and G9 formed from 1-, 2- and 4-arm copolymers, respectively, featuring a constant PEGMEMA:PPGMA ratio of 2:1. The results showed that 1-arm linear copolymer exhibited a sol-gel transition at 25 °C assessed by the switch between G' and G'', while the 2- and 4-arm

PHB based copolymers exhibited a storage modulus always higher than the loss modulus from 0 to 50 °C. G1 exhibited a classic thermoresponsive behavior typical of polymers composed with PNIPAAM and PPG segments.[23] In fact, at low temperature, core-shell micelles were formed due to the amphiphilic character of the copolymer, PNIPAAM and PPGMA then became more hydrophobic at 25 °C providing the driving force to form aggregated micelles ultimately resulting in a physical gel. After increasing the temperature to 32 °C, the NIPAAM LCST (Lower Critical Solution Temperature) was reached which resulted in a high increase of G' and G'' values due to the collapse and aggregation of the previously formed micelles. The gels formed with 2- and 4-arm copolymers also showed a thermoresponsive behavior. Temperature sweep experiment showed that the gels formed exhibited high G' and G'' values when PNIPAAM LCST was reached, thus suggesting the formation of gels with strong mechanical properties at body temperature (37 °C) as illustrated in Figure 6.

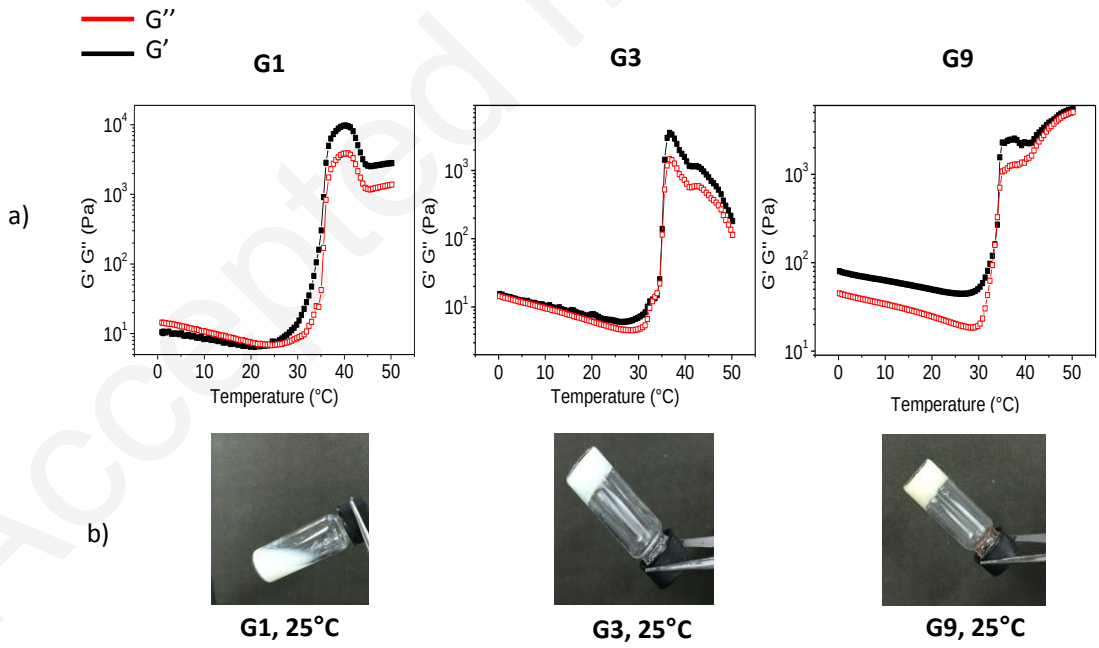


**Figure 6.** a) Rheological data from oscillatory measurements plotted as storage and loss moduli (G' and G'') versus temperature obtained from temperature sweep measurements done on G1, G3 and G9 gels (Table 3, entries 1, 3, 9). b) Pictures showing the effect of the number

of arms on the gelation properties on G1, G3 and G9 gels (Table 3, entries 1, 3, 9), respectively, formed with P1: $PHB1_{1400}$-*b*-$PNIPAAM_{6000}$-*b*-($PPEGMEMA_{9900}$-*co*-$PPPGMA_{5200}$), P2: $PHB2_{2500}$-*b*-$PNIPAAM_{7000}$-*b*-($PPEGMEMA_{9900}$-*co*-$PPPGMA_{5200}$), and P5: $PHB4_{1700}$-*b*-$PNIPAAM_{5000}$-*b*-($PPEGMEMA_{9900}$-*co*-$PPPGMA_{5200}$) (Table 1, entries 1, 2, 5).

In order to evaluate the influence of the number of arms in PHB-*b*-PNIPAAM-*b*-(PPEGMEMA-*co*-PPPGMA) on the viscoelastic properties of the supramolecular formed hydrogels, oscillation frequency sweep measurements were carried out at a strain of 0.2% which was determined as the linear-viscoelastic region by oscillation amplitude sweep measurements (Figure 7a). The storage modulus (G') and loss modulus (G'') were monitored over the strain frequency. The magnitude of the gel storage modulus is about $10^4$ Pa which is about the modulus of skeletal muscle.[24] At low frequencies, the gels exhibited very low G' and G'' values and then reached a plateau at a strain frequency of 20 $s^{-1}$. At higher frequencies, G1 and G3 gels presented very high values of G' and G'', thus evidencing their high stability with a solid-like behavior resulting in highly structured materials at this state. As expected, the number of arms significantly affected the mechanical properties, with G' and G'' values of the gel formed with the 1-arm copolymer being 10 times lower than those obtained for the gels formed from 2- and 4-arm copolymers. The G9 gel displayed a behavior assimilated to a fluid-like material, with a tendency to lose its mechanical properties at high frequency. Despite the linear structure of the P2 copolymer, the gel formed presented a similar behavior as the gel obtained with the 4-arm PHB with slightly lower values of G' and G''. This result suggested that the linear or star-shaped topology of the copolymer was not the only chemical characteristic that governed the gel solidity. The chemical structure of the 2-arm copolymer seemed to enhance the stability and the mechanical properties of the gel

compared to the 1-arm copolymer, with hydrophobic interactions most likely favored by this structure.

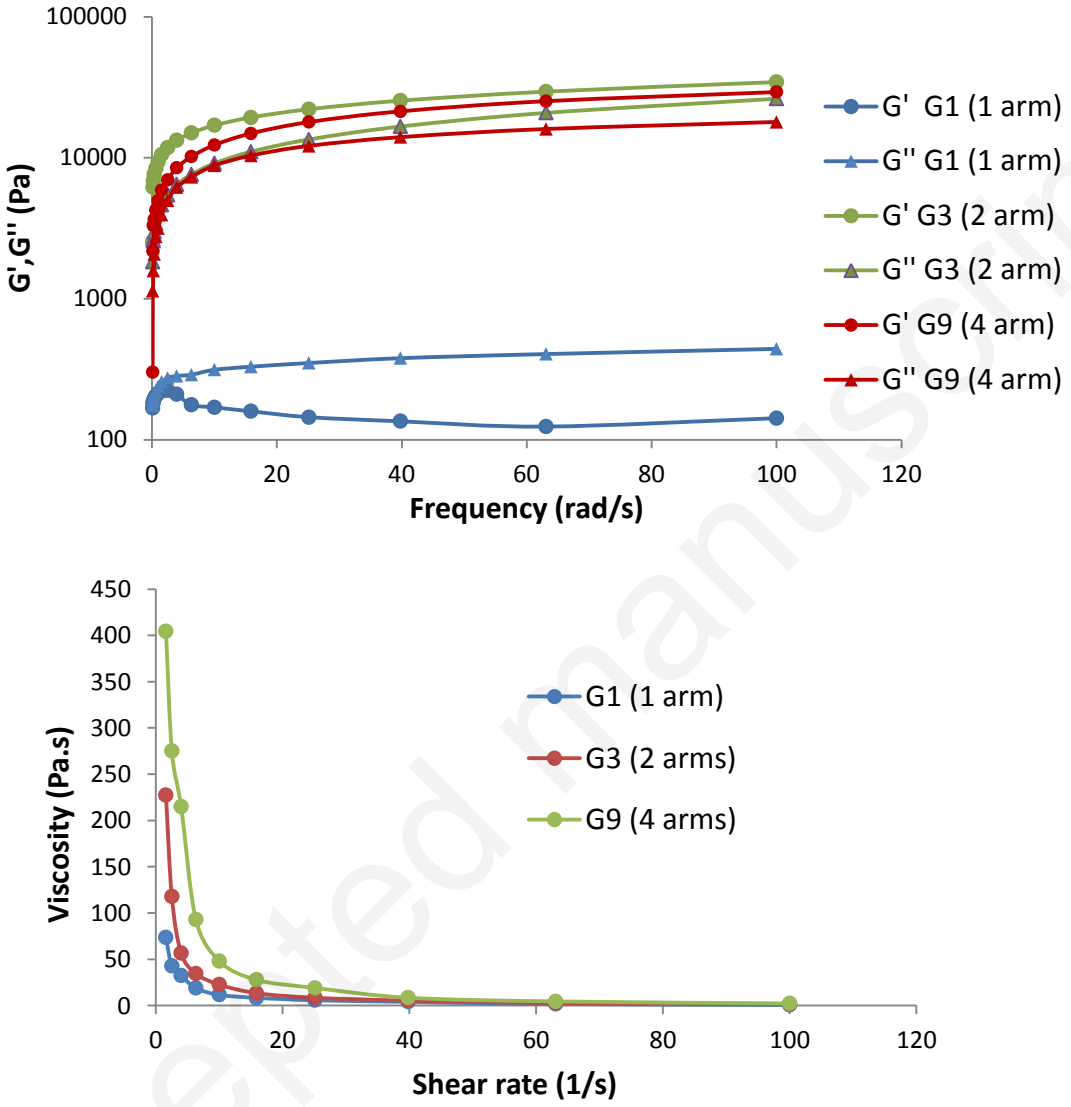


**Figure 7.** a) Rheological data from oscillatory measurements plotted as storage and loss moduli (G' and G'') versus frequency and b) apparent viscosity ($\eta_{app}$) versus shear rate obtained from flow measurements (at 37 °C) done on gels G1, G3 and G9 (Table 3, entries 1, 3, 9) respectively formed with P1: PHB1$_{1400}$-*b*-PNIPAAM$_{6000}$-*b*-(PPEGMEMA$_{99000}$-*co*-PPPGMA$_{5200}$), P2: PHB2$_{2500}$-*b*-PNIPAAM$_{7000}$-*b*-(PPEGMEMA$_{99000}$-*co*-PPPGMA$_{5200}$), and P5: PHB4$_{1700}$-*b*-PNIPAAM$_{5000}$-*b*-(PPEGMEMA$_{99000}$-*co*-PPPGMA$_{5200}$ ); Table 1, entries 1, 2, 5).

Furthermore, the rheological properties were evaluated by flow sweep measurements at 37 °C. As the shear rate increased, the viscosity started to decrease and the materials became more fluid. The swift drop of the viscosity suggested the loss of some mechanical properties when the shear rate increased, a behavior making the gel potentially injectable in a human body. Once again, the number of arms affected the rheological properties. Indeed, the viscosity increased with the number of arms over the whole range of applied shear rate (from 0 to 100 $s^{-1}$). It is also interesting to note that, unlike the poly(PEG/PPG/PHB urethane)s reported by our group[2e, 2f, 25], these gels are not transparent. These gels are also more susceptable to synerisis, resulting in a collapsed gel when the temperature is raised beyond 55 $^{o}$C. However, this gel appears to be more stable than other types of PNIPAAM-based polymers reported previously in literature which collapse after storage for a few days.[26]

**Drug release studies.** To demonstrate the potential utility of multi-arm based PHB copolymers as drug delivery systems, a model anticancer drug, doxorubicin, was next encapsulated in the formed gels and the drug release was studied in phosphate buffer saline (PBS, pH 7.4) at 37 °C. As shown in Figure 8, the doxorubicin release profile of the PHB-based hydrogels showed a two-stage pattern with a fast drug release rate within the initial 50 h followed by a plateau with a maximum of 80% release after 140 h of incubation. The number of arms significantly affected the drug-release profile. Indeed, only 50% of the drug was released after 140 h from gels G3 and G9 formed with the 2- and 4-arm copolymers, respectively, while 80% of doxorubicin was released with the micellar solution formed with the 1-arm copolymer-based gel G1. Gels G9 and G3 exhibited a slow release profile thus making these promising as long term drug delivery systems. As the data suggested, the number of arms significantly affected the rate of drug release due to the difference in micellar network structure (Figure 9). G3 and G9 which were prepared by using 2-arm and 4-arm

copolymers, consisted of micellar networks with more entanglement and bridging chains at the corona as compared with G1 linear structure. Thus, drug release from these polymeric networks (G3 and G9) were more restricted. This is coherent with the drug release results reported previously on PEG/PPG/PHB thermogels[27], using linear triblock PEG-PPG-PEG copolymer gel as the control. Complete drug release from PEG-PPG-PEG copolymer gel was observed in 4 h, while the PEG/PPG/PHB thermogels consisting of micellar network entanglement and bridging chains, showed slower release which lasted 40 days. The effect of hydrophilic/hydrophobic balance of the gel was also studied. PEGMEMA:PPGMA ratio also significantly impacted the release profile. The gel G7 based on the 2-arm polymer with such a ratio equal to 4:1 (P4) exhibited the slowest release with only 35% doxorubicin released after 140 h due to the higher affinity between the gel and doxorubicin in the PEG hydrophilic corona. As demonstrated, the drug release kinetic profile of doxorubicin can easily be tuned by first varying the number of arms in the copolymer, and also by the hydrophilic fraction of the copolymer. These results make these copolymers valuable for a large range of biomedical applications.

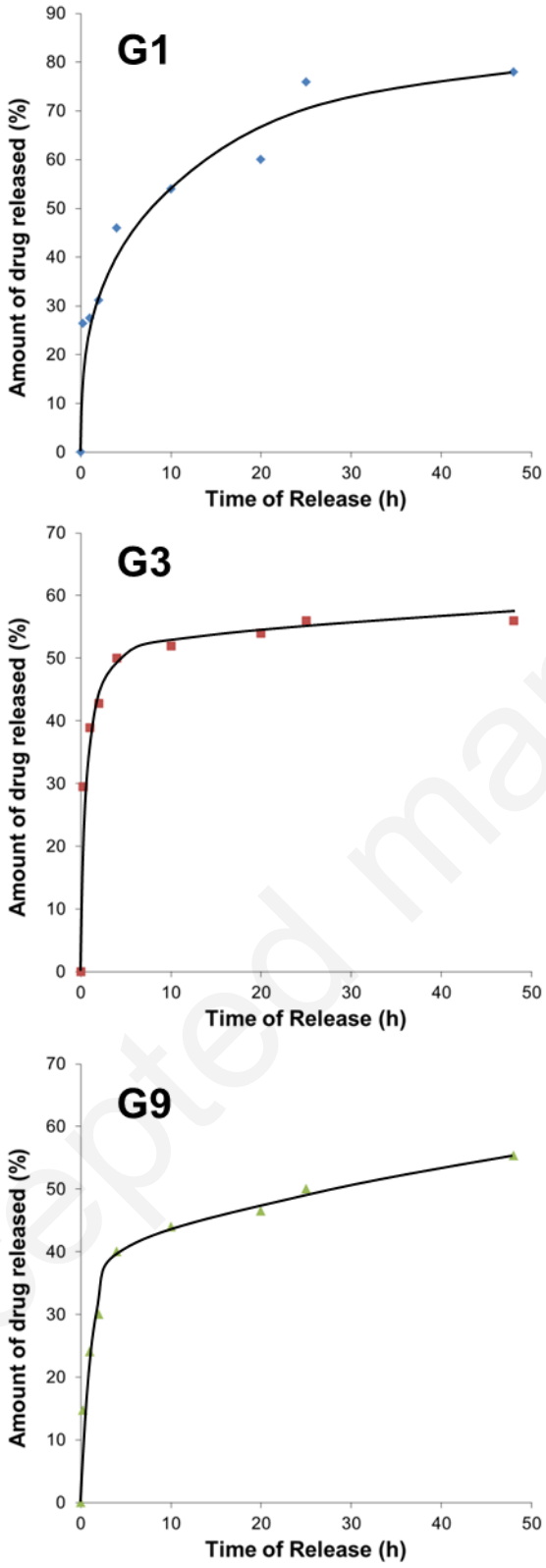


**Figure 8.** Drug release profile of hydrogels G1,G3 and G9 in PBS at 37 °C (Table 3, entries 1, 3,9), respectively, formed with P1: PHB$1_{1400}$-*b*-PNIPAAM$_{6000}$-*b*-(PPEGMEMA$_{9900}$-*co*-

PPGMA$_{5200}$), P2: PHB2$_{2500}$-*b*-PNIPAAM$_{7000}$-*b*-(PPEGMEMA$_{9900}$-*co*-PPPGMA$_{5200}$), and P5: PHB4$_{1700}$-*b*-PNIPAAM$_{5000}$-*b*-(PPEGMEMA$_{9900}$-*co*-PPPGMA$_{5200}$) (Table 1, entries 1, 2, 5).

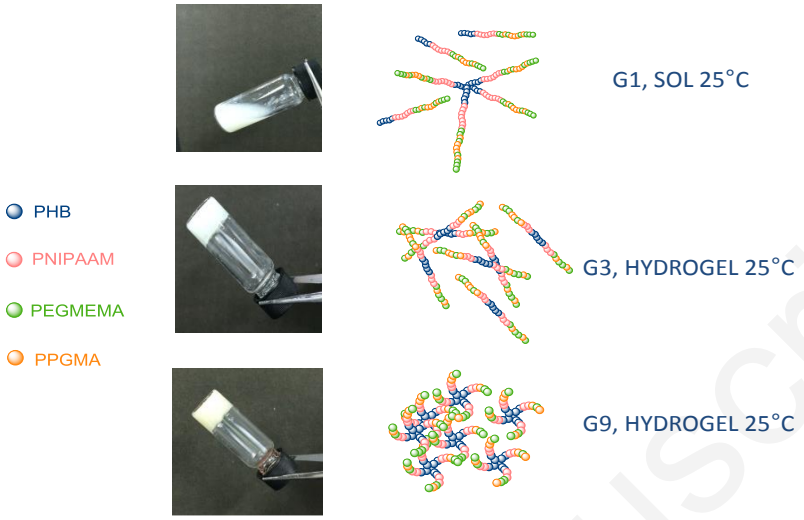


**Figure 9.** Schematic drawing of the proposed micellar network structure of G1, G3 and G9.

**Cytotoxicity of PHB based hydrogel.** In order to consider these gels as potential drug delivery systems, the biological safety aspect of the copolymers was assessed. The cytotoxicity was evaluated by incubating the CCD-112CoN human fibroblast cell lines with different concentrations of the copolymer solutions over a period of 24 h at 37 °C. Quantification of the cytotoxic response was performed using the MTT assay, as shown Figure 10. No significant toxic response was observed even at a high concentration of 1 mg.mL$^{-1}$, a promising value for the future development of temperature-responsive biomaterials based on these multi-arm PHB copolymers. Only the G5 gel seemed to reduce the cell viability, but in this case, the $IC_{50}$ (50% inhibitory concentration) being over 1 mg.mL$^{-1}$, it cannot preclude the use of this copolymer in some biomedical applications. The chemical topology of the copolymers did not seem to affect the cells viability.

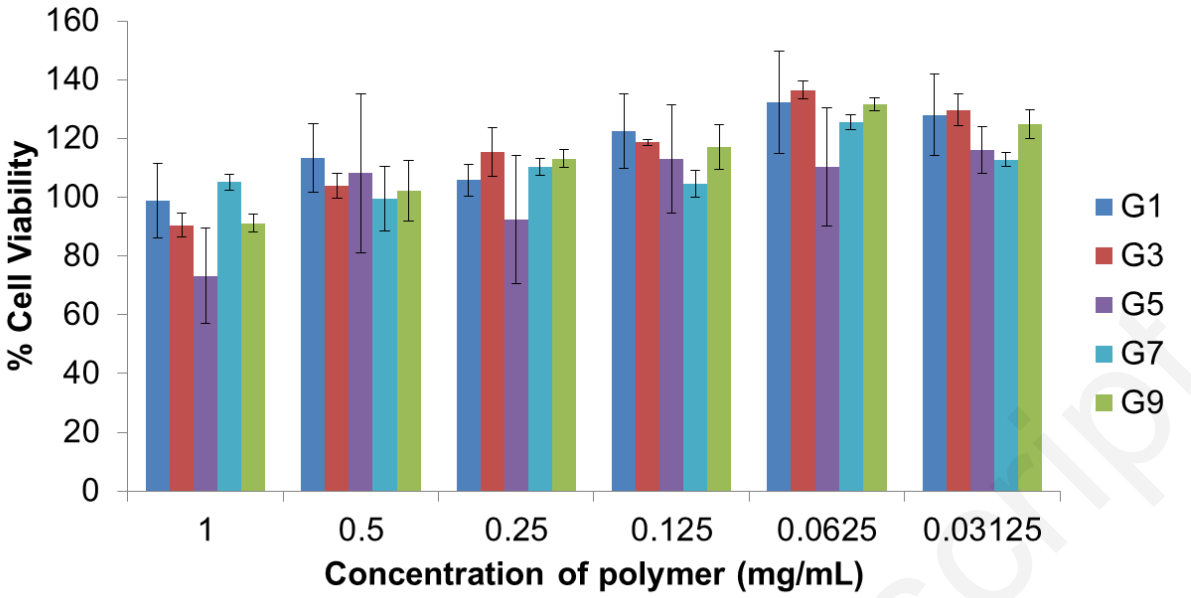


**Figure 10.** Cell viability of CCD-112CoN human fibroblast cell lines incubated with G1, G3, G5, G7 and G9 gels (Table 3, entries 1, 3, 5, 7, 9) respectively formed with P1: PHB$1_{1400}$-*b*-PNIPAAM$_{6000}$-*b*-(PPEGMEMA$_{9900}$-*co*-PPPGMA$_{5200}$), P2: PHB$2_{2500}$-*b*-PNIPAAM$_{7000}$-*b*-(PPEGMEMA$_{9900}$-*co*-PPPGMA$_{5200}$), P3: PHB$2_{2500}$-*b*-PNIPAAM$_{5700}$-*b*-(PPEGMEMA$_{7700}$-*co*-PPPGMA$_{7500}$), P4: PHB$2_{2500}$-*b*-PNIPAAM$_{4600}$-*b*-(PPEGMEMA$_{12100}$-*co*-PPPGMA$_{3000}$), and P5: PHB$4_{1700}$-*b*-PNIPAAM$_{5000}$-*b*-(PPEGMEMA$_{9900}$-*co*-PPPGMA$_{5200}$) (Table 2, entries 1–5) with a range of concentration varying from 0.03 to 1 mg.L$^{-1}$.

## Conclusion

Original linear and star-shaped PHB-based amphiphilic triblock copolymers, PHB-*b*-PNIPAAM-*b*-(PPEGMEMA-*co*-PPPGMA) were synthesized from the successive ATRP of NIPAAM, and PEGMEMA and PPGMA, using bromoesterified PHB macroinitiators. Copolymers with 1, 2 and 4 arms featuring PPEGMEMA:PPPGMA ratio varying from 1:1 to 4:1 were prepared in grams quantity and characterized by $^{1}$H and $^{13}$C[$^{1}$H] J-MOD NMR, TGA and DSC analyses.

These amphiphilic copolymers formed hydrogels in water at a minimal concentration of 15% (*w/v*). The effect of the number of arms and hydrophilic/hydrophobic content on the rheological properties were assessed by rotational flow sweep, oscillation frequency sweep and oscillation temperature sweep measurements. Formed hydrogels revealed a tunable thermoresponsive behavior due to PNIPAAM and PPG segments. The modulus of gels varied according to the number of arms of the copolymers. The gels formed from 2- and 4-arm copolymers exhibited interesting mechanical properties as highly structured gels with solid-like behavior, while the 1-arm PHB copolymer formed micellar solution. These various types of supramolecular structures could be used as originals biocompatible drug delivery systems as illustrated by doxorubicin release profile and by the absence of cytotoxicity towards human fibroblasts cell lines.

**Experimental section**

**Materials**

PHB ($M_n$ = 59 400 g.mol$^{-1}$), poly(ethylene glycol) methyl ether methacrylate (PEGMEMA, $M_n$ = 1100 g.mol$^{-1}$), poly(propylene glycol) methacrylate (PPGMA, $M_n$ = 375 g.mol$^{-1}$), *N*-isopropylacrylamide (NIPAAM, $M_n$ = 113 g.mol$^{-1}$), hexanol, ethylene glycol, erythritol, 1,4-dioxane (anhydrous, 99.8%), α-bromoisobutyryl bromide, 1,1,4,7,10,10-hexamethyl-triethylenetetramine (HMTETA, 97.0%), copper(I) bromide (CuBr > 98.0%), and all other reagents, were purchased from Sigma-Aldrich and used as received unless otherwise stated. Triethylamine was purchased from Fischer Scientific and used as received. PPGMA stabilized with mono methyl ether hydroquinone (MEHQ) as inhibitor was purified through the appropriate inhibitor remover column before use. NIPAAM was purified by two successive recrystallizations from hexane and drying overnight under dynamic vacuum. CuBr was successively washed with acetic acid and acetone, and finally degassed with $N_2$ before use. Spectra/Por dialysis membranes with a molecular weight cut off (MWCO) of 3500 g.mol$^{-}$1

(nominal flat width = 45 mm, diameter = 29 mm, volume/length = 15 m/50 ft) were purchased from Spectrumlabs.

**Instrumentation and measurements**

Size exclusion chromatography (SEC) measurements were performed on a Waters GPC system equipped with Waters Styragel columns, a Waters-2420 ELS detector, at 40 °C. HPLC grade THF was used as the eluent at a low flow rate of 1.0 mL.min$^{-1}$. The (co)polymer samples were dissolved in THF (2 mg mL$^{-1}$). Monodispersed PMMA standards ($M_n$ range = 580–380 000 g.mol$^{-1}$) were used to generate the calibration curve; all $M_{n,SEC}$ values of the (co)polymers were uncorrected for their potential difference in hydrodynamic radius vs. PMMA.

$^{1}$H (400 MHz) and $^{13}$C[$^{1}$H] J-MOD (100 MHz) NMR spectra were recorded on Bruker Ascend 400 spectrometer at 25 °C and were referenced internally relative to $SiMe_4$ (δ 0 ppm) using the residual solvent resonance. Chemical shifts (δ) are reported in ppm and were referenced internally relative to tetramethylsilane (δ 0 ppm) using the residual $^{1}$H and $^{13}$C solvent resonances.

Molar mass values of PHBs-OH and PHBs-Br were determined from $^{1}$H NMR spectra of the precipitated polymer sample in $CDCl_3$ from the relative intensities of the resonances of the main-chain methine hydrogens (–OC*H*($CH_3$)$CH_2$CO, δ 5.26 ppm), to the methyl end-group hydrogens (–O($CH_2$)$_5$C*H*$_3$, δ 0.87 ppm), or the methylene hydrogens (–OC*H*$_2$C*H*$_2$ δ 4.25 ppm) of ethylene glycol, or the methylene hydrogens (–OC*H*$_2$CH, δ ca. 4.00 ppm) of erythritol, for 1-, 2- and 4-arm PHBs, respectively, with $M_{3\text{-hydroxybuturate}}$ = 86 g.mol$^{-1}$. The good resolution of the resonances corresponding to the various transesterification alcoholic reagents allowed their fairly reliable integration (Figures S1–S6).

The NIPAAM conversion was determined from $^{1}$H NMR analysis of the crude copolymer samples in $CDCl_3$ by using the integration (Int.) ratio Int.$_{PNIPAAM}$/[Int.$_{PNIPAAM}$ +

Int.$_{NIPAAM}$] of the methine hydrogens (–NC*H*($CH_3$)$_2$, $\delta_{NIPAAM}$ 3.99 ppm, $\delta_{PNIPAAM}$ 4.14 ppm) of NIPAAM/PNIPAAM (Table 1). The molar mass values of PNIPAAM block in PHB-*b*-PNIPAAM copolymers were determined by $^1$H NMR analysis in $CDCl_3$, from the relative intensities of the signals of the methylene (–$CH_2$CH(CONH($CH_3$)$_2$), δ 2.51 ppm) to the PHB main-chain methine hydrogens (–OCH($CH_3$)C*H*$_2$, δ 5.26 ppm) as previously determined for PHB-Br before addition of NIPAAM. Since the molar mass value of PPEGMEMA-*co*-PPPGMA block could not be determined from the $^1$H NMR spectra due to the overlap of their respective characteristic signals, the experimental molar mass values were considered to be equal to the theoretical molar mass data assuming the quantitative conversion of PEGMEMA and PPGMA. The resonance of the methylene hydrogens of both PEGMEMA and PPGMA monomers (C*H*$_2$C($CH_3$)C(O)–, δ 5.51, 6.02 ppm, respectively) totally disappeared after the appropriate polymerization time as shown Figure 3.

Thermogravimetric analyses (TGA) were performed on a TA Instrument Q500 apparatus. Samples were initially heated at 20 °C.min$^{-1}$ from 25 °C to 700 °C in a dynamic nitrogen atmosphere with a flow rate of 70 mL.min$^{-1}$. Decomposition temperatures were taken at the peak maximum of the first derivative of weight remaining (%) against temperature (°C) curve.

Differential scanning calorimetry (DSC) measurements were carried out on a TA Instruments Q100. Each sample was analyzed at a rate of 10 °C.min$^{-1}$, under continuous flow of helium (25 mL.min$^{-1}$), using aluminum capsules. The thermograms were recorded according to the following cycles: –30 °C to 170 °C at 20 °C.min$^{-1}$, 170 °C for 2 min, 170 °C to –30 °C at 5 °C.min$^{-1}$, and finally –30 °C to 170 °C at 5 °C.min$^{-1}$. Data were collected during the second heating cycle.

The rheological behavior of the hydrogels was studied using a dynamic hybrid rheometer (DHR-3) (TA instrument, USA) with 40-mm stainless steel flat plate geometry.

Temperature cooling was controlled by a thermocube circulation system attached to the peltier plate. A rotational flow sweep was carried out to measure the viscosity of the hydrogels at 37 °C, with shear rate range of 1–100 $s^{-1}$. An oscillation amplitude sweep was performed to determine the linear visco-elastic region (LVR) of all the systems, with a fixed frequency of 1 Hz, and a variable strain ranging from 0.02 to 100% at 37 °C. An oscillation frequency sweep was carried out to examine the modulus change in response to frequency ranging from 0.1 to 100 Hz, with a fixed strain at 2% at 37 °C. It should be noted that both the amplitude and frequency sweeps give the storage modulus (G') and the loss modulus (G'') of the hydrogels, but under different environments. An oscillation temperature sweep was used to determine the gelation temperature of the systems, with a controlled ramp rate of 2 °C.$min^{-1}$, from 0 to 70 °C. The experiment was carried out at low strain (0.2 %) and low frequency (1 Hz) to ensure that the gelation process does not interfere under these conditions. The sol-gel transition point was monitored from the point at which G' and G" intersect.[28]

**Synthesis of multi-arm PHBs as ATRP macroinitiators.** The mono-hydroxylated PHB or 1-arm PHB (PHB1-OH), was synthesized from the transesterification of commercially available high molar mass (59 400 g.$mol^{-1}$) PHB, according to the previously reported procedure.[18] The resulting α-hydroxy telechelic PHB, PHB1-OH was thus isolated (Table S1). $^1$H NMR (400 MHz, $CDCl_3$, 23 °C) δ (ppm) 5.25 (m, 18H, C(O)$CH_2$C*H*($CH_3$)O), 4.18 (br s, 1H, $CH_2$CH($CH_3$)O*H*), 4.08 (t, 2H, $CH_3(CH_2)_4CH_2$OC(O)), 2.52 (d of m, 42H, C(O)C*H*$_2$CH($CH_3$)O), 1.27–1.25 (m, 70H, C(O)$CH_2$CH(C*H*$_3$)O, $CH_3(CH_2)_4CH_2$OC(O)), 0.85 (br t, 3H, C*H*$_3$($CH_2$)$_4$$CH_2$OC(O); Figure S1).

PHB1-OH was then bromoesterified into PHB1-Br to be next used as an ATRP macroinitiator. The purified PHB1-OH (1.50 g, 0.90 mmol, 1 equiv.) was dissolved in dry THF (20 mL), and triethylamine (0.21 g, 2.1 mmol, 2.4 equiv.) was added into the reaction flask placed at 0 °C. α-Bromoisobutyryl bromide (0.40 g, 1.76 mmol, 2 equiv.) dissolved in

dry THF (10 mL) was next added dropwise into the cold reaction mixture, and the reaction was stirred for 24 h (reaction times were not systematically optimized). The resulting polymer was precipitated in cold diethylether and washed several times with water and then acetone until complete elimination of residual diglyme to afford PHB1-Br ($M_{n,NMR}$ = 1400 g.mol$^{-1}$; Table S1, Figure S4). $^{1}$H NMR (400 MHz, $CDCl_3$, 23 °C) δ (ppm) 5.25 (m, 17H, C(O)$CH_2$C*H*($CH_3$)O), 4.08 (t, 2H, $CH_3(CH_2)_4CH_2OC(O)$), 2.52 (d of m, 35H, C(O)C*H*$_2$CH($CH_3$)O), 1.85 (br s, 1HOC(O)C($CH_3$)$_2$Br), 1.27–1.23 (m, 60H, C(O)$CH_2$CH(C*H*$_3$)O, $CH_3(CH_2)_4CH_2OC(O)$), 0.85 (br t, 3H, $CH_3(CH_2)_4CH_2OC(O)$; Figure S4).

The dihydroxylated PHB or 2-arm PHB (PHB2-OH), was synthesized similarly to PHB1-OH, from the transesterification of commercially available high molar mass (59 400 g.mol$^{-1}$) PHB (9.5 g, 0.16 mmol, 1 equiv.) using ethylene glycol (2.99 g, 48 mmol, 300 equiv.) and DBTL(0.15 mL, 0.16 g, 0.25 mmol, 1.5 equiv.) (Table S1, entry 2). The reaction mixture was then stirred for 24 h at 140 °C. The resulting PHB was next precipitated in diethylether and dried under vacuum overnight to afford α,ω-dihydroxy telechelic PHB2-OH ($M_{n,NMR}$ = 2300 g.mol$^{-1}$, Figure S2). PHB2-OH was then bromesterified following the same procedure as described above with PHB1-OH, to afford PHB2-Br ($M_{n,NMR}$ = 2500 g.mol$^{-1}$; Table S1, Figure S5).

The tetra-hydroxylated PHB or 4-arm PHB (PHB4-OH), was synthesized following the same procedure as described above for the preparation of the 1-arm PHB, by using PHB (11.9 g, 0.20 mmol, 1 equiv.), erythritol (7.32 g, 60 mmol, 300 equiv.) and DBTL (0.15 mL, 0.16 g, 0.25 mmol, 1.2 equiv.) (Table S1, entry 3). α,ω-Tetrahydroxy telechelic PHB ($M_{n,NMR}$ = 1700 g.mol$^{-1}$; Figure S3) was then brominated following the same procedure as described for the 1-arm PHB to afford PHB4-Br ($M_{n,NMR}$ = 1700 g.mol$^{-1}$; Figure S6).

**Synthesis of PHB-*b*-PNIPAAM-*b*-(PPEGMEMA-*co*-PPPGMA).** The formation of the triblock copolymers was carried out according to a two-step ATRP approach. In a typical experiment, PHB1-Br (1.4 g, 1 mmol, 51 equiv.), HMTETA (69 mg, 0.3 mmol, 1.5 equiv.), and NIPAAM (2.3 g, 20 mmol, 100 equiv.) were introduced in a reaction flask and dissolved in dioxane (5 mL) (Table 1, entry 1). After degassing the reaction mixture with nitrogen over 30 min, CuBr (29 mg, 0.2 mmol, 1 equiv.) was added under nitrogen, and the mixture again degassed with nitrogen during 10 min before reaction for 24 h. The NIPAAM conversion (55–89%) was then measured by $^{1}$H NMR in $CDCl_3$ prior to the addition of PEGMEMA and PPGMA. Quantitative conversion of NIPAAM was not targeted in order to lower the polymerization time and to limit the extent of side reactions. Unreacted NIPAAM was removed from the isolated PHB-*b*-PNIPAAM-*b*-(PPEGMEMA-*co*-PPPGMA) triblock copolymers upon dialysis (see below). A prepared dioxane (1 mL) solution of PPGMA (1.3 g, 3.5 mmol, 14 equiv.) and PEGMEMA (2.4 g 2.2 mmol, 9 equiv.), previously degassed with nitrogen during 10 min, was then added into the reaction mixture under inert atmosphere. The mixture was then stirred for 24 h and then eluted through a basic alumina column using THF (300 mL). This recovered solution was then concentrated using a rotary evaporator, and the copolymer was next dissolved in acetone (20 mL) and dialyzed for 48 h with a dialysis membrane (MWCO of 3500 g.mol$^{-1}$) using acetone (800 mL) which was renewed twice in order to eliminate any residual PHB–OH, NIPAAM, PPGMA, PEGMEMA. Careful drying of the copolymer afforded the desired PHB-*b*-PNIPAAM-*b*-(PPEGMEMA-*co*-PPPGMA) in > 50% typical yield (ca. 4 g, 0.17 mmol, Figures 3,S7,S8). This approach enabled to tune the composition of the copolymers by simply changing the feeding composition of the monomers. A series of PHB-*b*-PNIPAAM-*b*-(PPEGMEMA-*co*-PPPGMA) with a different number of PHB arms and different PEGMEMA/PPGMA ratios was thus prepared. The number-average molar mass and dispersity values of the triblock copolymers measured by SEC are reported in Table 1.

**Preparation of PHB-*b*-PNIPAAM-*b*-(PPEGMEMA-*co*-PPPG) gels.** In a typical procedure, the selected PHB-*b*-PNIPAAM-*b*-(PPEGMEMA-*co*-PPPGMA) copolymer (200 mg) was dissolved in distilled water (1 mL), stirred over 30 min and then placed in an ultrasound bath for 15 min. The gel formed was then left overnight at room temperature to equilibrate. A gel with a concentration of 20% (*w/v*) was then recovered and next used for rheological studies. The gel concentrations of 15% (*w/v*) were also evaluated (Figure S9).

**Doxorubicin release study.** An aqueous solution (Phosphate Buffer Saline (PBS), 0.5 mL) containing 20wt% of the PHB-*b*-PNIPAAM-*b*-(PPEGMEMA-*co*-PPPGMA) copolymer and doxorubicin (0.5 mg) was prepared in a test-tube. The mixture was stirred for 30 min and then left in an ultrasound bath during 15 min. The gel formed was then left to equilibrate over 2 h at room temperature and then placed at 37 °C during the appropriate time. At a predetermined time-interval, an aliquot of the buffer (100 µL) was extracted and replaced with the same volume of fresh PBS. Each test was reproduced three times. The 100 µL sample buffer extracted was used to determine the doxorubicin concentration by measuring the UV absorbance at $\lambda$ = 480 nm.

**Cytotoxicity study of the copolymers.** The cytotoxicity of the polymers was evaluated using the thiazolyl blue tetrazolium bromide MTT assay in CCD-112CoN human fibroblast cell lines cultured in complete medium. The cells were seeded in a 96-well plate at a density of 2 × $10^4$ cells/well grown overnight before being incubated in polymer solutions at a serial concentration of 1000, 500, 250, 125, 62.5 and 31.3 µg.mL$^{-1}$ in complete medium over 24 h at 37 °C. The cell viability was assessed with the MTT assay and the absorbance was measured using a microplate reader (Infinite M200, Tecan) at a wavelength of 570 nm. The cell viability (%) was calculated relative to the control cells cultured in medium without polymers.

**Acknowledgements**

The authors gratefully thank Rennes Metropole (mobility grant to G.B.), the Fondation pour la Recherche Médicale (FRM, PhD grant to G.B.), and A*STAR and IMRE (mobility grant to G.B.). L.S.S. would like to thank Dr. Zhang Zhongxing and Dr. Li Zibiao for advice in NIPAAM purification and polymerization. L. X. J. acknowledges the A*STAR Personal Care Programme Grant.

## References


[1] aM. D. Segarra-Maset, B. Escuder, J. F. Miravet, *Chemistry-a European Journal* **2015**, *21*, 13925-13929; bJ. Shi, D. Yuan, R. Haburcak, Q. Zhang, C. Zhao, X. Zhang, B. Xu, *Chemistry-a European Journal* **2015**, *21*, 18047-18051; cM. Wallace, A. Z. Cardoso, W. J. Frith, J. A. Iggo, D. J. Adams, *Chemistry-a European Journal* **2014**, *20*, 16484-16487; dL. Qin, F. Xie, P. Duan, M. Liu, *Chemistry-a European Journal* **2014**, *20*, 15419-15425.

[2] aD. Mandal, S. K. Mandal, M. Ghosh, P. K. Das, *Chemistry-a European Journal* **2015**, *21*, 12042-12052; bS. Nummelin, V. Liljestrom, E. Saarikoski, J. Ropponen, A. Nykanen, V. Linko, J. Seppala, J. Hirvonen, O. Ikkala, L. M. Bimbo, M. A. Kostiainen, *Chemistry-a European Journal* **2015**, *21*, 14433-14439; cH. Wang, S. Song, J. Hao, A. Song, *Chemistry-a European Journal* **2015**, *21*, 12194-12201; dM. S. Thompson, M. V. Tsurkan, K. Chwalek, M. Bornhauser, M. Schlierf, C. Werner, Y. Zhang, *Chemistry-a European Journal* **2015**, *21*, 3178-3182; eY.-L. Wu, X. Chen, W. Wang, X. J. Loh, *Macromolecular Chemistry and Physics* **2016**, *217*, 175-188; fS. S. Liow, Q. Dou, D. Kai, A. A. Karim, K. Zhang, F. Xu, X. J. Loh, *ACS Biomaterials Science & Engineering* **2016**, *2*, 295-316; gZ. Li, P. L. Chee, C. Owh, R. Lakshminarayanan, X. J. Loh, *RSC Adv.* **2016**, *6*, 28947-28955; hD. Kai, M. J. Tan, P. L. Chee, Y. K. Chua, Y. L. Yap, X. J. Loh, *Green Chem.* **2016**, *18*, 1175-1200.

[3] aB. Jeong, Y. H. Bae, S. W. Kim, *Journal of Controlled Release* **2000**, *63*, 155-163; bL. Yu, Z. Zhang, J. Ding, *Macromolecular Research* **2012**, *20*, 234-243; cM. Boffito, P. Sirianni, A. M. Di Rienzo, V. Chiono, *Journal of biomedical materials research. Part A* **2015**, *103*, 1276-1290.

[4] aK. L. Fujimoto, Z. Ma, D. M. Nelson, R. Hashizume, J. Guan, K. Tobita, W. R. Wagner, *Biomaterials* **2009**, *30*, 4357-4368; bZ. Li, X. Guo, S. Matsushita, J. Guan, *Biomaterials* **2011**, *32*, 3220-3232.

[5] aY. S. Chen, P. C. Tsou, J. M. Lo, H. C. Tsai, Y. Z. Wang, G. H. Hsiue, *Biomaterials* **2013**, *34*, 7328-7334; bT. Shimizu, M. Yamato, A. Kikuchi, T. Okano, *Biomaterials* **2003**, *24*, 2309-2316.

[6] aZ. Zhang, J. Ni, L. Chen, L. Yu, J. Xu, J. Ding, *Biomaterials* **2011**, *32*, 4725-4736; bT. Y. Ci, L. Chen, L. Yu, J. D. Ding, *Scientific Reports* **2014**, *4*.

[7] aH. J. Moon, Y. Ko du, M. H. Park, M. K. Joo, B. Jeong, *Chemical Society reviews* **2012**, *41*, 4860-4883; bX. J. Loh, J. Li, *Expert Opin. Ther. Patents* **2007**, *17*, 965-977; cQ. Q. Dou, S. S. Liow, E. Y. Ye, R. Lakshminarayanan, X. J. Loh, *Advanced Healthcare Materials* **2014**, *3*, 977-988; dE. Caló, V. V. Khutoryanskiy, *European Polymer Journal* **2015**, *65*, 252-267; eA. Vashist, A. Vashist, Y. K. Gupta, S. Ahmad, *Journal of Materials Chemistry B* **2014**, *2*, 147-166; fR. Dong, Y. Pang, Y. Su, X. Zhu, *Biomater Sci* **2015**, *3*, 937-954; gM. K. Nguyen, D. S. Lee, *Macromolecular bioscience* **2010**, *10*, 563-579.

[8] aX. J. Loh, S. H. Goh, J. Li, *Biomacromolecules* **2007**, *8*, 585-593; bJ. Li, X. Li, X. Ni, K. W. Leong, *Macromolecules* **2003**, *36*, 2661-2667; cX. J. Loh, Z.-X. Zhang, Y.-L. Wu, T. S. Lee, J. Li, *Macromolecules* **2009**, *42*, 194-202; dX. J. Loh, S. H. Goh, J. Li, *J. Phys. Chem. B* **2009**, *113*, 11822-11830.

[9] X. J. Loh, L. W. I. Cheng, J. Li, *Macromolecular Symposia* **2010**, *296*, 161-169.

[10] W. S. Shim, J. H. Kim, H. Park, K. Kim, I. Chan Kwon, D. S. Lee, *Biomaterials* **2006**, *27*, 5178-5185.

[11] aB. Jeong, Y. H. Bae, S. W. Kim, *Macromolecules* **1999**, *32*, 7064-7069; bL. Yu, G. Chang, H. Zhang, J. Ding, *Journal of Polymer Science Part A: Polymer Chemistry* **2007**, *45*, 1122-1133.

[12] aH. Zhang, L. Yu, J. Ding, *Macromolecules* **2008**, *41*, 6493-6499; bM. J. Hwang, J. M. Suh, Y. H. Bae, S. W. Kim, B. Jeong, *Biomacromolecules* **2005**, *6*, 885-890.

[13] aG. Q. Chen, *Chemical Society reviews* **2009**, *38*, 2434-2446; bM. N. Somleva, O. P. Peoples, K. D. Snell, *Plant biotechnology journal* **2013**, *11*, 233-252.

[14] aS. Taguchi, T. Iwata, H. Abe, Y. Doi, *Polym. Sci.: A Comprehensive Ref.* **2012**, 157-182; bJ. Lu, R. C. Tappel, C. T. Nomura, *Polymer Reviews* **2009**, *49*, 226-248; cK. Sudesh, H. Abe, Y. Doi, *Progress in Polymer Science* **2000**, *25*, 1503–1555; dR. W. Lenz, R. H. Marchessault, *Biomacromolecules* **2005**, *6*, 1-8.

[15] I. Noda, R. H. Marchessault, M. Terada, *Polymer Data Handbook*, Oxford University Press, New York, **1999**.
[16] K. L. Liu, J.-l. Zhu, J. Li, *Soft Matter* **2010**, *6*, 2300.
[17] T. Ebrahimi, S. G. Hatzikiriakos, P. Mehrkhodavandi, *Macromolecules* **2015**, *48*, 6672-6681.
[18] aT. Hirt, P. Neuenschwander, U. Suter, *Macromol. Chem. Phys.* **1996**, *197*, 1609-1614; bL. Jiang, S. S. Liow, X. J. Loh, *Polym. Chem.* **2016**, *7*, 1693-1700.
[19] S.-G. Hong, H.-W. Hsu, M.-T. Ye, *Journal of Thermal Analysis and Calorimetry* **2012**, *111*, 1243-1250.
[20] T. Toraman, B. Hazer, *Journal of Polymers and the Environment* **2014**, *22*, 159-166.
[21] P. J. Barham, A. Keller, E. L. Otun, P. A. Holmes, *Journal of Materials Science* **1984**, *19*, 2781-2794.
[22] M. Nuopponen, J. Ojala, H. Tenhu, *Polymer* **2004**, *45*, 3643-3650.
[23] aB. Diao, Z. Zhang, J. Zhu, J. Li, *RSC Adv.* **2014**, *4*, 42996-43003; bX. J. Loh, Y.-L. Wu, W. T. Joseph Seow, M. N. Irzuan Norimzan, Z.-X. Zhang, F.-J. Xu, E.-T. Kang, K.-G. Neoh, J. Li, *Polymer* **2008**, *49*, 5084-5094.
[24] K. Tan, S. Cheng, L. Jugé, L. E. Bilston, *Journal of Biomechanics* **2015**, *48*, 3788-3795.
[25] aX. J. Loh, S. H. Goh, J. Li, *Journal of Physical Chemistry B* **2009**, *113*, 11822-11830; bX. J. Loh, S. H. Goh, J. Li, *Biomacromolecules* **2007**, *8*, 585-593; cX. J. Loh, S. H. Goh, J. Li, *Biomaterials* **2007**, *28*, 4113-4123.
[26] G. T. Eom, S. Y. Oh, T. G. Park, *Journal of Applied Polymer Science* **1998**, *70*, 1947-1953.
[27] X. J. Loh, S. H. Goh, J. Li, *Biomaterials* **2007**, *28*, 4113-4123.
[28] aX. J. Loh, H. X. Gan, H. Wang, S. J. E. Tan, K. Y. Neoh, S. S. J. Tan, H. F. Diong, J. J. Kim, W. L. S. Lee, X. T. Fang, O. Cally, S. S. Yap, K. P. Liong, K. H. Chan, *Journal of Applied Polymer Science* **2014**, *131*; bX. J. Loh, W. Guerin, S. M. Guillaume, *Journal of Materials Chemistry* **2012**, *22*, 21249-21256; cV. P. N. Nguyen, N. Y. Kuo, X. J. Loh, *Soft Matter* **2011**, *7*, 2150-2159; dX. J. Loh, P. N. N. Vu, N. Y. Kuo, J. Li, *Journal of Materials Chemistry* **2011**, *21*, 2246-2254.